Eur. Phys. J. Appl. Phys. (2013) 63: 14407
DOI: 10.1051/epjap/2013120483

THE EUROPEAN PHYSICAL JOURNAL
APPLIED PHYSICS

Regular Article

Scaling prospects in mechanical energy harvesting with piezo nanowires*

Gustavo Ardila[a], Ronan Hinchet, Mireille Mouis, and Laurent Montès

IMEP-LAHC, Joint Research Unit, CNRS/Grenoble-INP/Université Joseph Fourier/Université de Savoie Grenoble-INP/Minatec, 3 parvis Louis Néel, Grenoble, France

Received: 22 October 2012 / Accepted: 9 April 2013
Published online: 5 July 2013 –

Abstract. The combination of 3D processing technologies, low power circuits and new materials integration makes it conceivable to build autonomous integrated systems, which would harvest their energy from the environment. In this paper, we focus on mechanical energy harvesting and discuss its scaling prospects toward the use of piezoelectric nanostructures, able to be integrated in a CMOS environment. It is shown that direct scaling of present MEMS-based methodologies would be beneficial for high-frequency applications only. For the range of applications which is presently foreseen, a different approach is needed, based on energy harvesting from direct real-time deformation instead of energy harvesting from vibration modes at or close to resonance. We discuss the prospects of such an approach based on simple scaling rules.

1 Introduction

The improvement of the energetic autonomy of future nano- and microsystems by harvesting energy from the environment is a topic of growing interest in the scientific and industrial community. Energy can be harvested from sources such as incident light, heat, radiofrequency, vibrations or mechanical impacts [1]. This strategy can lengthen battery autonomy in mobile applications, which are currently one of the largest markets in telecommunications. In other applications, such as sensor networks, where the energy requirement is evaluated ideally to about 100 μW [2], energetic autonomy would provide a number of advantages: it would allow energy supply wiring to be suppressed while avoiding the additional maintenance costs due to the replacement or charging of batteries. For large sensor networks, wiring would anyway be impossible due to weight, cost and reliability issues. On the other hand, battery management can be very complicated when the sensors are not easily accessible.

Mechanical energy harvesting, in particular, has been extensively studied and reported in the literature using MEMS technologies [3]. Three main approaches have been proposed: electromagnetic, electrostatic and piezoelectric approaches. At the nanoscale, only the piezoelectric approach has been studied and some devices have been reported [4–6].

In this paper, we will focus on the harvesting of mechanical energy using piezoelectric materials. After having recalled the principle of energy harvesting using MEMS structures, we will discuss the consequences of device scaling down and show that a change of paradigm is necessary to harvest energy from nanostructures in the range of frequencies of interest for most present fields of applications. This has the additional advantages of extending the bandwidth, suppressing the need for high quality factors and allowing energy harvesting from random signals such as those arising from human activity.

2 Energy harvesting using resonant MEMS

At microscale, the most widely used device architecture for mechanical energy harvesting consists in a seismic mass placed at the end of a piezoelectric beam. Beam deformation produces an electric potential difference which is converted into electrical energy. This system realizes a mechanical resonator, the design of which is optimized to increase energy transfer at a given resonance frequency. The aim is to increase the quality factor (Q) of the resonator, but at the expense of a narrower bandwidth [1].

The energy density reported for MEMS piezoelectric devices is typically in the range of 0.1 mW/cm^3 to 40 mW/cm^3 [1] at low frequency (<150 Hz) and input accelerations between 1 m/s^2 and 10 m/s^2 corresponding to an applied force between ∼30 μN and ∼40 mN. For industrial applications, two commercial solutions are presently provided by Midé and Perpetuum. Several monitoring integrators, such as General Electrics, are using

* Contribution to the Topical Issue "International Semiconductor Conference Dresden-Grenoble – ISCDG 2012", Edited by Gérard Ghibaudo, Francis Balestra and Simon Deleonibus.

[a] e-mail: ardilarg@minatec.inpg.fr

Table 1. Piezoelectric coefficient d_{33} in nanostructured materials compared to bulk.

Material	d_{33} [pm/V]		
	Theoretical (nanoscale)	Experimental (nanoscale)	Experimental (bulk)
PVDF	N/A	−38 [10]	−25
PZT	N/A	101 [6]	650
ZnO	168.2 [11]	14–26.7 [9]	9.93
GaN	65.8 [11]	12.8 [21]	1.86
PMN-PT	N/A	381 [12]	2500 [12]

their power supply solution in wireless sensors for rotating machines. The main issues are price, volume, bandwidth and minimum input acceleration. Typical devices from Midé and Perpetuum deliver 15 V with a power density of 9 mW/cm^3, and 5 V with 20 mW/cm^3, respectively. The bandwidth is rather narrow (50–150 Hz) and the minimum acceleration is about 1 m/s^2. In principle, resonant oscillators can only harvest energy in a narrow band of frequencies, while most real applications provide mechanical inputs with a wider frequency spectrum. As reviewed in [7], many techniques have been proposed to overcome this issue, such as, for instance, arrays of structures with different resonant frequencies, amplitude limiters, coupled oscillators, nonlinear springs, bi-stable structures and large inertial masses with a high degree of damping.

At MEMS scale, many piezoelectric materials have been studied: from natural crystals like quartz, compound semiconductors such as nitrides (AlN for example), oxides such as PZT ($Pb(Zr_xTi_{1-x})O_3$) and polymers such as PVDF (polyvinylidene fluoride) [1]. These materials are generally available in the form of ceramics, composites or thin polycrystalline layers. The materials with the best figure of merit are bulk ceramics, such as PZT. Unfortunately, their integration is not straightforward. Therefore, despite they not showing as good properties as ceramics yet, thin semiconducting nitride layers are widely studied in the literature because of their easier integration into MEMS [8].

3 Energy harvesting using piezoelectric nanostructures

In this section, the most studied piezoelectric materials at the nanoscale are presented, showing their advantages compared to bulk materials. Then, two approaches to harvest mechanical energy using nanostructures are presented: a resonant approach, based on MEMS cantilevers and a nonresonant approach. Their advantages and disadvantages are discussed. Finally the efficiency of the mechanical to energy conversion at the nanoscale is discussed as well as further possible improvements using engineered nanostructures.

3.1 Piezolectric nanomaterials

Presently, the piezoelectric materials which are mostly studied at nanoscale are ZnO [9], PVDF [10], GaN [11], PZT [6] and PMN-PT [12], ZnO being the material of choice for most investigations, it can be fabricated easily at low temperatures with a larger range of structures and dimensions but their properties cannot be modified easily [13–16]. GaN is a very interesting material as it offers better integration prospects with Si and both *n*- and *p*-type doping can be achieved, heterostructures can also be obtained [17–20]. As shown in Table 1, which displays reported values of the d_{33} coefficient (longitudinal, along *c*-axis), most of these materials have their piezoelectric properties improved at nanoscale. This is an advantage if used in sensors or energy harvesting systems.

3.2 Scaling down of resonant devices toward nanometer scale

For this study, we used cylindrical nanowires of length L and diameter D as model nanostructures. Their resonance frequency (f) can be evaluated from cantilever mechanics as:

$$f = \frac{3.52D}{8\pi L^2}\sqrt{\frac{E}{\rho}}, \tag{1}$$

where E is the Young's modulus and ρ is the mass density [22]. The effect of scaling is displayed in Figure 1. Reducing the diameter decreases the resonance frequency linearly, while reducing the length or reducing the general size (diameter and length in the same proportion) induces a sharp increase of the resonance frequency.

For a typical 50 nm wide, 1 μm long GaN nanowire (NW), the resonance frequency is found close to 20 MHz. In this calculation, we used recent evaluations of the Young modulus and mass density, obtained from direct measurement using an AFM probe, with values of 44 GPa and 6.15 kg/m^3 respectively [23]. Such a resonance frequency is too high for most present applications of mechanical energy harvesting, for which the range of frequencies of use is below 200 Hz from human body and some structures and around a few kilohertz from machines vibrations [1].

The energy provided by a single NW being very small (typically 10 to 20 pW for a reference ZnO NW [24]), energy harvesting systems must be based on an ensemble of NWs. It is interesting to evaluate how the resonance frequency would change in such a case. The modeled structure is depicted in Figure 2 where vertical NWs are connected to a seismic mass. This kind of structure has been proposed in [25] and further realized, without considering any resonance effect, in [4].

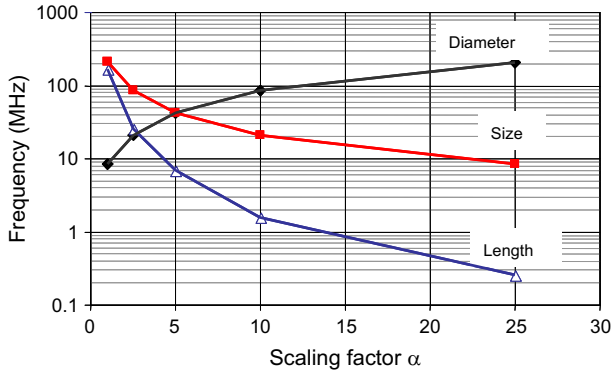

Fig. 1. Effect of the reduction of size on the resonance frequency of a cantilever. The reference device ($\alpha = 1$) is a 10 nm wide and 1 μm long nanowire (NW) on the diameter study, 10 nm wide and 200 nm long NW on the size study and finally 50 nm wide, 500 nm long NW on the length study.

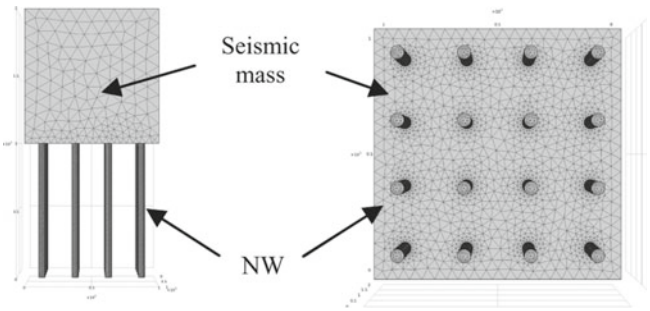

Fig. 2. Side view and top view of the elementary cell simulated to calculate the resonance frequency of an array of vertical NWs connected by a seismic mass. The NWs are considered as fully clamped to a solid substrate at their bottom. The seismic mass is supposed to be made of tungsten.

Simulations based on the finite element method (FEM) were used to calculate the influence on the resonance frequency of such parameters as the area of the array, the density of NWs (number of NWs per unit area) and the value of the seismic mass. Calculations were performed for ZnO. It was found that the simulation of a 1 μm^2 area was sufficient to represent the response of larger devices. Our reference structure consisted of a 100 NW/μm^2 array with 1 μm long NWs and a 1 μm thick seismic mass. This density corresponds to 50 nm wide NWs spaced by 50 nm. As shown in Figure 3, the resonance frequency can be decreased by increasing the thickness of the seismic mass or by reducing the density of NWs. However, it seems difficult to reach resonance frequencies lower than several kHz. A resonance frequency of 6 kHz was obtained for a density of 4 NWs/μm^2 and 100 μm thick seismic mass. While it effectively increases output power, arranging NWs into resonant arrays should not provide a large design margin in terms of resonance frequency.

The general conclusion from these simulations is that the resonance frequency would remain high. Resonance-based modes are not the most appropriate at low frequency. A better approach consists in considering real-time deformations, as considered in the next section.

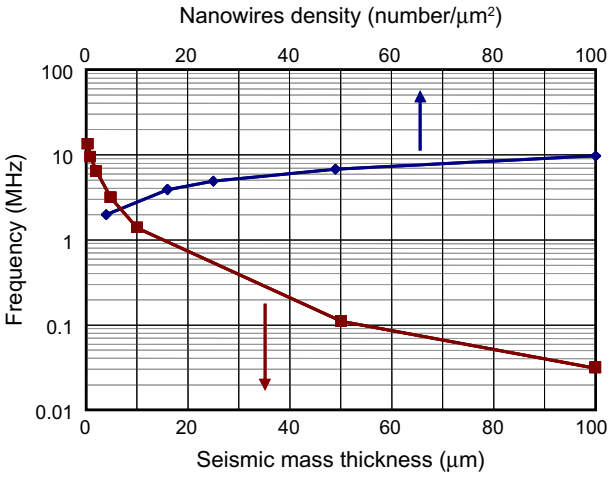

Fig. 3. Resonance frequency of the structure as a function of (a) thickness of the seismic mass and (b) number of NWs per μm^2.

These deformations could be encountered in low-frequency applications (some machines) or when random mechanical inputs are available (human body) [1].

3.3 Scaling rules for nonresonant nanostructures

In this section, we will develop scaling rules for nonresonant nanobeams, based on classical mechanics. As a first approach, we considered several hypotheses in order to derive simple analytical expressions: (i) nonlinear effects are neglected, (ii) the main contribution to the strain would be in the axial axis. Our reference device is a 50 nm wide and 1 μm long ZnO NW. The scaling factor α was applied to the diameter, to the length or to both diameter and length (this case will be referred to as a change in size). In the following, we consider single clamped nanowires under bending conditions. The derived expression from classical mechanics for the strain (S), deformation (dz) and stiffness (κ) using the hypotheses stated above can be defined as [22]:

$$S = \frac{4FL}{\pi E r^3}, \tag{2}$$

$$dz = \frac{FL^3}{3EI_y}, \tag{3}$$

$$\kappa = \frac{3EI_y}{L^3}, \tag{4}$$

where F is the vertically applied force, r is the radius of the NW and I_y is the quadratic moment of a cylinder defined as:

$$I_y = \frac{\pi r^4}{4}. \tag{5}$$

Figure 4 shows the influence of size scaling on axial strain (Eq. (2)), axial deformation (Eq. (3)) and stiffness (Eq. (4)). Stiffness, which depends on Young's modulus and geometrical parameters, is linearly decreasing as size

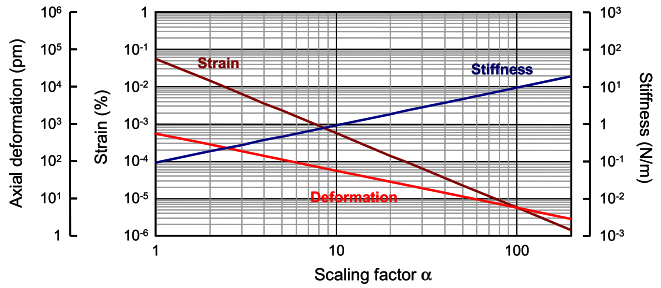

Fig. 4. Effect of the size scaling down of a cantilever in terms of axial strain, axial deformation and stiffness under fixed force (80 nN).

decreases, allowing much larger strains to be reached under fixed force. This is directly beneficial to the piezoelectric potential. The associated deformation does not increase as quickly as the force is applied to a shorter beam. The maximal strain on the nanobeam increases greatly as the size is reduced, as will be shown below, this will improve the energy generated from a single nanobeam. The main conclusion is that a smaller force is sufficient to produce a given voltage.

To evaluate the efficiency of the mechanical to electrical energy conversion of a nonresonant structure, let us consider the energy variation between two, strained and unstrained, states. The mechanical energy W stored in strained state can be expressed as [22]:

$$W = \frac{1}{2} E S^2 V, \tag{6}$$

where V is the volume. The electrical energy generated in the piezoelectric material when deformed can be defined as [6]:

$$E_c = \frac{1}{2} E^2 \frac{d_{33}^2 S^2}{\varepsilon} V, \tag{7}$$

where ε is the dielectric constant. In this expression, we consider as a first approach that the main contribution to the energy generation is given by the d_{33} piezoelectric coefficient; this will produce an underestimation of the energy generated of five times if a lateral force is applied [26], but will give us useful insight into the scaling rules. The efficiency of energy conversion (electromechanical coupling factor) can be deduced from these two equations as

$$\eta = \frac{E_c}{W} = E \frac{d_{33}^2}{\varepsilon}, \tag{8}$$

which is independent of geometrical factors. Equation (8) was used to study scaling properties of the power density for a mechanical harvesting device integrating ZnO NWs. The active area was fixed to 1 cm^2 and the overall basis thickness to 500 μm plus the length of the NWs. A homogeneous distribution of NWs was considered, with a distance equal to their diameter. For comparison with present MEMS devices, we assumed 50 mechanical deformations (not necessarily periodic) per second. The results are displayed in Figure 5, where NWs with larger diameters than

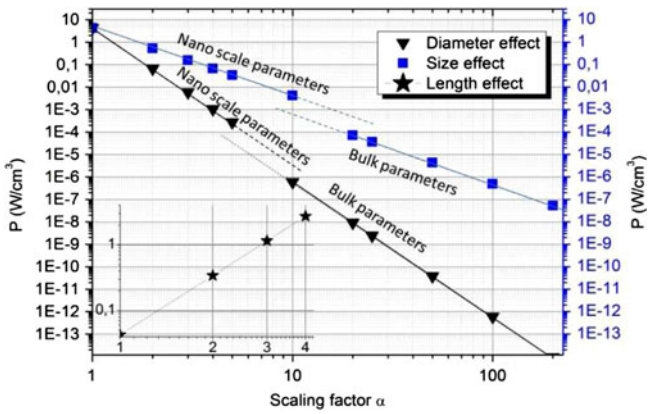

Fig. 5. Power density of a mechanical energy harvesting device based on vertically integrated ZnO NWs. Effect of diameter and size scaling down (main graph) and of length scaling down (inset), with a constant force equal to 10 nN or 1 nN, respectively.

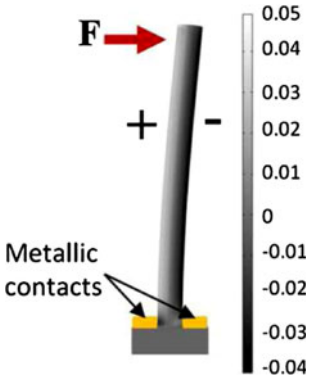

Fig. 6. FEM simulation of a ZnO NWs (50 nm wide, 600 nm long) showing the voltage at its surface as it bends under a force of 25 nN. Positive charges are created at the region under tension, negative charges are created at the region under compression.

300 nm are supposed to have bulk properties based on experimental results on ZnO and GaN NWs [9,21].

Nanowires size and diameter downscaling result in power density increase. The theoretical value for the smallest device (4 W/cm^3 for $\alpha = 1$) is comparable to that of present MEMS devices, while requiring a much smaller force (10 nN is sufficient here). The corresponding power, which reaches 2 mW for one square centimeter, becomes compatible with the power needed to feed future autonomous systems ($\sim$100 μW) [2]. Increasing the length of the NWs also increases power density (in this case a smaller force of 1 nN was considered to remain in the small deformations regime). It should be noted that scaling down is also beneficial to reduce the overall weight.

An important issue would be how to place the electrical contacts to collect the charges generated when the NWs bent. FEM simulations coupling mechanical and piezoelectric properties (Fig. 6) show that positive charges are created in the region under tension and negative charges in the region under compression. One possible way to recover

Table 2. Efficiency of energy conversion for different nanostructured materials. Apart from the dielectric constant, material parameters are experimental values at nanoscale.

Material	Material parameter			
	d_{33} [pm/V]	E [GPa]	$\varepsilon/\varepsilon_0$ (Bulk)	Efficiency
PVDF	−38 [10]	0.39 [29]	13 [6]	0.005
PZT	101 [6]	46.4–99.3 [30]	300–1300 [6]	0.09–0.18
ZnO	14–26.7 [6]	100 [31]	10.9 [6]	0.2–0.7
GaN	12.8 [21]	43.9 [23]	8.9	0.09

the charges on individual NWs would be placing metallic contacts at the bottom of the NW [27]. These contacts could be placed using Nano-imprint techniques, E-beam lithography or interference lithography [28], before the selective growth of the NWs.

This is not the only way to integrate NWs into mechanical harvesting devices. Several devices integrating piezoelectric nanostructures working at low frequency (<10 Hz) have been reported. Vertically grown ZnO NWs have been integrated reporting up to 2.7 mW/cm^3 [4]. In this device, the metallic contacts are placed at the bottom (before the NWs growth) and at the top by sputtering, after the immersion of the NWs into a PMMA matrix. Lateral ZnO NWs have been integrated on a flexible substrate after growth, and then lateral metallic contacts equally distributed have been placed using lift-off. The reported power density is 2V@11 mW/cm^3 [5]. Very recently PZT nanoribbons have been integrated laterally on a polymer, and have shown the highest reported piezoelectric coefficients (Tab. 1) but when integrated into devices they reach 0.25V@10 nW/cm^2 at 3 Hz [6], showing clearly that integration needs to be improved. In this last device, lateral contacts have been placed equally distributed using photolithography and wet etching.

3.4 Materials comparison for nonresonant harvesting

Based on equation (4), Table 2 compares typical parameters reported in the literature for some piezoelectric nanostructures, assuming that ε keeps its bulk value as a first approximation. This table shows that ZnO presents the best efficiency for energy conversion, although GaN presents a higher improvement in this parameter compared to the bulk materials (evaluated to ∼0.013 [27]).

3.5 Further possible improvements at nanoscale

The piezoelectric properties of nanostructures can be further improved, with resulting increase of energy harvesting efficiency. Indeed, recent qualitative measurements on 25 nm wide, 500 nm long GaN NWs featuring an 8 nm AlN barrier along their axis resulted in an estimated value of the effective piezoelectric coefficient which was nine times larger than for their GaN intrinsic counterparts [32]. This would increase the efficiency of energy conversion by a factor 81, leading to 10 times improvement compared to ZnO. Although this theoretical prediction might be alleviated by integration details such as contact quality or process-induced size dispersion [4], the use of heterostructured NWs is undoubtedly opening very interesting prospects.

4 Conclusions

Because of their improved properties, such as enhanced piezoelectric coefficients and reduced stiffness, piezoelectric nanostructures are a promising solution for mechanical energy transduction into electrical energy. This can be used to harvest mechanical energy from environment in the perspective of feeding autonomous systems, as well as for sensing applications.

It has been shown however that for low-frequency applications, nanostructures should not be operated in the resonant or close to resonance modes, and should rather be operated in real-time deformation mode. This is important for wearable applications or structural health monitoring, where mechanical inputs are random or at very low frequency (from fractions of Hz to kHz). Each single deformation event is then generating a small amount of energy. It should be noted that the force needed to induce a deformation is decreasing with device downscaling so that the probability of such events is increasing. It has been shown that the energy provided by an array of NWs could be compatible with the power needed to feed future autonomous systems. Using heterostructured NWs can further increase the energy conversion efficiency.

This work has been partly supported by the European Union 7th Framework Program, within the Network of Excellence NanoFunction under Grant Agreement FP7/ICT/NoE No. 257375. Partial support was received also from UJF Grenoble (SMINGUE).

References

1. K.A. Cook-Chennault, N. Thambi, A.M. Sastry, Smart Mater. Struct. **17**, 043001 (2008)
2. A. Nechibvute, A. Chawanda, P. Luhanga, Smart Mater. Res. 2012 (2012)
3. P.D. Mitcheson, E.M. Yeatman, G.K. Rao, A.S. Holmes, T.C. Green, Proc. IEEE **96**, 1457 (2008)
4. S. Xu et al., Nanotechnology **5**, 366 (2010)

5. G. Zhu, R. Yang, S. Wang, Z.L. Wang, Nano Lett. **10**, 3151 (2010)
6. Y. Qi, M.C. McAlpine, Energy Environ. Sci. **3**, 1275 (2010)
7. D. Zhu, M.J. Tudor, S.P. Beeby, Meas. Sci. Technol. **21**, 022001 (2010)
8. M. Marzencki, Y. Ammar, S. Basrour, Sens. Actuators A **145–146**, 363 (2008)
9. M.H. Zhao, Z.L. Wang, S.X. Mao, Nano Lett. **4**, 587 (2004)
10. C. Chang, V.H. Tran, J. Wang, Y.-K. Fuh, L. Lin, Nano Lett. **10**, 726 (2010)
11. R. Agrawal, H.D. Espinosa, Nano Lett. **11**, 786 (2011)
12. S. Xu, G. Poirier, N. Yao, Nano Lett. **12**, 2238 (2012)
13. D. Yuan, R. Guo, Y. Wei, W. Wu, Y. Ding, Z.L. Wang, S. Das, Adv. Func. Mater. **20**, 3484 (2010)
14. X.D. Wang, J.H. Song, P. Li, J.H. Ryou, R.D. Dupuis, C.J. Summers, Z.L. Wang, J. Am. Chem. Soc. **127**, 7920 (2005)
15. S.S. Lin, J.I. Hong, J.H. Song, Y. Zhu, H.P. He, Z. Xu, Y.G. Wei, Y. Ding, R.L. Snyder, Z.L. Wang, Nano Lett. **9**, 3877 (2009)
16. S. Xu, Y.G. Wei, M. Kirkham, J. Liu, W.J. Mai, R.L. Snyder, Z.L. Wang, J. Am. Chem. Soc. **130**, 14958 (2008)
17. Z. Zhong, F. Qian, D. Wang, C.M. Lieber, Nano Lett. **3**, 343 (2003)
18. R. Songmuang, O. Landré, B. Daudin, Appl. Phys. Lett. **91**, 251902 (2007)
19. C.-T. Huang, J. Song, W.-F. Lee, Y. Ding, Z. Gao, Y. Hao, L.-J. Chen, Z.L. Wang, J. Am. Chem. Soc. **132**, 4766 (2010)
20. B. Alloing, S. Vézian, O. Tottereau, P. Vennéguès, E. Beraudo, J. Zuniga-Péreza, Appl. Phys. Lett. **98**, 011914 (2011)
21. M. Minary-Jolandan, R.A. Bernal, I. Kuljanishvili, V. Parpoil, H.D. Espinosa, Nano Lett. **8**, 970 (2012)
22. W. Young, R. Budynas, *Roark's Formulas for Stress and Strain*, 7th edn. (McGraw-Hill, 2002)
23. H. Ni, X. Li, G. Cheng, R. Klie, J. Mater. Res. **21**, 11 (2006)
24. P.X. Gao, J. Song, J. Liu, Z.L. Wang, Adv. Mater. **19**, 67 (2007)
25. A.R. Abramson et al., J. Micro. Systems **13**, 3 (2004)
26. Y.F. Gao, Z.L. Wang, Nano Lett. **7**, 2499 (2007)
27. R. Hinchet, J. Ferreira, J. Keraudy, G. Ardila, E. Pauliac-Vaujour, M. Mouis, L. Montès, in *IEEE International Electron Devices Meeting (IEDM), San Francisco, CA, 2012*
28. S.D. Hersee, X. Sun, X. Wang, Nano Lett. **6**, 1808 (2006)
29. R. Nakashima, K. Watanabe, Y. Lee, B.-S. Kim, I.-S. Kim, Adv. Pol. Tech. **32**, E44 (2011)
30. X. Chen, A. Li, N. Yao, Y. Shi, Appl. Phys. Lett. **99**, 193102 (2011)
31. S. Hoffmann et al., Nanotechnology **18**, 205503 (2007)
32. X. Xu et al., Nanotechnology **22**, 105704 (2011)